FERMILAB-PUB-16-249-TD (accepted)

Mu2e Transport Solenoid Prototype Design and Manufacturing

P. Fabbricatore, G. Ambrosio, S. Cheban, D. Evbota, S. Farinon, M. Lamm, M. Lopes, R. Musenich, R. Wands, G. Masullo

***Abstract*—The Mu2e Transport Solenoid consists of fifty-two coils arranged in twenty-seven coil modules that form the S-shaped cold mass. Each coil is wound from Al-stabilized NbTi superconductor. The coils are supported by an external structural aluminum shell machined from a forged billet. Most of the coil modules house two coils with the axis of each coil oriented at an angle of approximately five degrees with respect to each other. The coils are indirectly cooled with LHe circulating in tubes welded on the shell. In order to enhance the cooling capacity, pure aluminum sheets connect the inner bore of the coils to the cooling tubes. The coils are placed inside the shell by the means of a shrink fit procedure. A full-size prototype, with all the features of the full assembly, was successfully manufactured in a collaboration between INFN-Genoa and Fermilab. In order to ensure an optimal mechanical pre-stress at the coil-shell interface, the coils are inserted into the shell through a shrink fitting process. We present the details of the prototype with the design choices as validated by the structural analysis. The fabrication steps are described as well.**

***Index Terms*—Superconducting Magnets, Solenoids, Accelerator Magnets**

I. Introduction

THE experiment Mu2e, currently in the prototype phase at Fermilab, aims to observe the neutrinoless direct conversion of a muon to electron [1]. Pions generated by a proton beam colliding with a tungsten target decay into muons, which are transported to an Al target. The generation and transport of the muon beam is controlled through magnetic fields generated by two superconducting solenoids: the Production Solenoid (PS) and the Transport Solenoid (TS). The detectors, placed after the Al target, sit in the magnetic field generated by a third superconducting solenoid: the Detector Solenoid (DS).

The three superconducting solenoids constitute a critical component of the whole experiment in terms of both effort and cost [2].

This manuscript is focused on the superconducting modules of the TS [3], in particular the design and manufacturing aspects of a prototype module are discussed.

Detailed information about the TS can be found in Ref. [3].

Manuscript received October 19, 2015.

P.Fabbricatore (corresponding author; phone:+390103536340; e-mail pasquale.fabbricatore@ge.infn.it) , S.Farinon and R.Musenich are with INFN Sezione di Genova, I-16146 Genova, Italy..

G.Ambrosio, S.Cheban, D.Evbota,,M.Lamm, M.Lopes and R.Wands are with Fermi National Accelerator Laboratory, Batavia, IL 60510 USA

G.Masullo is with ASG Superconductors, Corso Perrone 73r Genova,Italy

In brief the TS is composed of 27 modules, most of them with two superconducting coils. They generate a magnetic field up to 2.5 T in a warm bore of 0.5 m. The TS has a serpentine (S) shape of 13.4 m length. The modules of the TS are not all equal, but the basic characteristics are almost the same: coils wound with a pure Al stabilized conductor are integrated inside an Al alloy shell, as shown in Fig. 1. The axis of each coil in a module is oriented at an angle of approximately five degrees with respect to the adjacent coil.

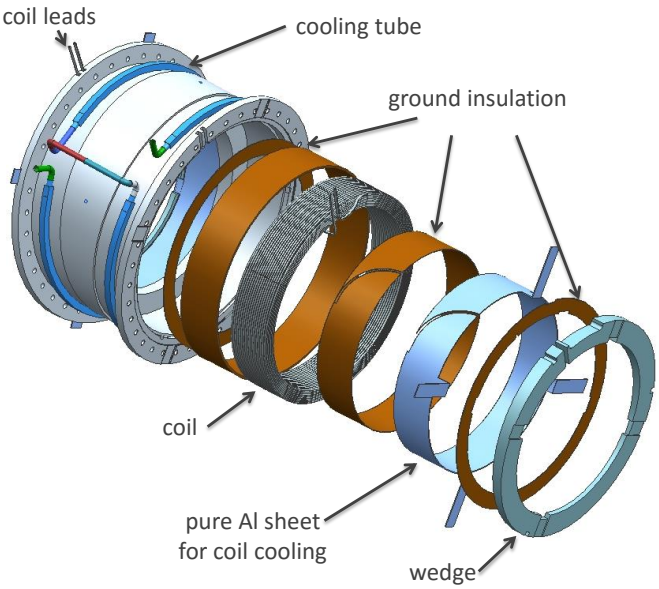

Fig. 1. Exploded view of a typical TS coil module, containing two superconducting coils. The different components associated with a single coil are shown. The cooling is indirect: LHe flows in pipes welded onto the shell.

The main problem we faced was how to integrate the coils in the shell in a way that would guarantee a solid mechanical fixing of the coils, so that they do not move under the action of magnetic forces so as to avoid premature quenches. It should be noted that in some modules the axial forces change direction when all three solenoids are powered as compared to when only the TS is powered.

This paper discusses the ideas developed for integrating coils and shell and how these ideas were put in practice with the construction of a prototype module.

II. Module Characteristics and Basic Design Considerations

The TS is divided into two sections: the Upstream (TSu) and Downstream (TSd) Solenoids . The main characteristics of

Operated by Fermi Research Alliance, LLC under Contract No. De-AC02-07CH11359 with the United States Department of Energy.

TSu are given in Table I. The TSd magnet has the same cable design and a slightly lower peak field and energy.

TABLE I
Main Parameters of TSu Magnet

Item	Unit	Value
Bore	m	0.93
Inductance	H	4.7
Energy	MJ	7.1
Operating current	A	1730
Peak field along magnet central axis	T	2.5
Peak coil field (B_{peak})	T	3.4
Peak coil temperature (T_{peak})	K	4.5
Operating current fraction on load line at T_{peak}		56%
Thermal margin at B_{peak}, T_{peak}	K	1.87

The conductor used in all the coils is an Al stabilized conductor obtained by co-extruding a multi-strand NbTi flat cable with high purity aluminum. The characteristics of the conductor are given in Table II.

This kind of conductor was developed in the past for detector magnets [4] because the conductor stability, expressed in terms of the so called minimum quench energy, is maximized by the use of very high purity Al (99.992% or better). For the Mu2e solenoids the stability argument was enhanced by the need to have a material that is able to recover from the residual resistivity ratio (RRR) damage caused by irradiation.

TABLE II
MAIN PARAMETERS OF TS CONDUCTOR

Symbol	Unit	Value
Strand (NbTi) diameter	mm	0.67
Number of strands		14
Cu/nonCu ratio in the strand		1
Initial RRR of Cu matrix/Al stabilizer		100/800
Al-stabilized cable width	mm	9.85
Al-stabilized cable thickness	mm	3.11
Cable critical current at 5 T, 4.2 K	A	5900

The TS was conceived as an S-shaped magnet with a modular structure [3]. Magnetic and mechanical constraints require a rigid mechanical structure containing the superconducting coils and precisely determining the S-shaped magnetic channel. One of the functions of the mechanical structure is to contain the magnetic forces generated by the TS coils and by the interaction of TS coils with PS and DS solenoids. Generally the shell of each module needs to provide the hoop strength and to prevent coil movements along the axial direction. To this purpose a good mechanical coupling between the shell and the winding is essential. The use of a pure Al stabilized conductor naturally led to choosing an Al alloy as shell material, as has been done with other superconducting detector magnets like CDF, BaBar, Aleph and others [5]. An Al alloy shell possesses good mechanical and thermal properties that well match those of a pure Al stabilized conductor. This thermal compatibility keeps almost unchanged the interface pressure between the coils and shell when cooling down from room temperature to 4.22 K.

The basic problem is how to guarantee an acceptable interface pressure between the superconducting coil and the shell. The most common technique for detector magnets involves the inner winding of the conductor inside the shell, followed by an under vacuum impregnation with an epoxy resin. The physical contact (with some radial interface pressure) between the coil and the shell is provided by the winding, whilst the bonding is guaranteed by the impregnation. For the TS solenoid this technique is not feasible due to the limited inner diameter of the coil (less than 1 m).

Another option consists in winding a coil, then impregnating it with an epoxy resin and precisely machining the external surface, creating a small gap between the external coil radius and the inner shell radius. This gap (tenths of millimeter) is filled with a charged resin. At first sight, this solution appears viable for the Mu2e modules. However, a closer study showed that this technique is more suitable for a copper stabilized conductor because the differential integral thermal contraction from room temperature to 4.2 K of copper and aluminum helps in radially pre-stressing the coil after cool-down. For a coil using an Al stabilized conductor, there is a risk in stressing by tension the epoxy layer filling the gap, thereby generating cracks in the resin and potential sources of instabilities during operations. In the worst case the contact between coil and shell could be lost, causing possible coil movement during the current ramp.

A way around this problem is to have a mechanical interference between the coil and shell. In this case the integration of the coil into the shell must be done with a shrink-fitting operation. Detector magnets like CDF and ZEUS were constructed with this technique. The shrink-fitting guarantees the desired pre-stress level of the coil, but the operation contains some risks. In order to insert the coil into the shell, the shell should be heated up to more than 120 ^{o}C, to generate a radial gap on the order of 1 mm. Under these conditions the coil, at room temperature, is inserted into the shell. In case the operation fails, the coil could be only partially inserted into the shell, requiring complex and very risky removal (by cutting or machining) of the shell.

For the Mu2e modules the above described risk is greatly reduced due to the relatively small axial length of the coils (less than 200 mm). At the same time there is an increased risk due to the need to shrink-fit two coils sequentially in the same shell. These considerations signaled the need to develop a prototype module for the purpose of testing the reliability of the construction method and assessing the extent of control over the mechanical coil pre-stressing. The module including coils #14 and #15 was chosen for construction of the prototype of the TSu because it was considered the best representative of all the modules of the TS. The coils have the geometrical characteristics given in Table III.

In the next section the mechanical analysis for evaluating the mechanical interference between the coils and shell is given as well as the methods and the tool designed for the shrink-fitting operation. Finally, the steps of the construction are briefly discussed.

TABLE III
GEOMETRICAL CHARACTERISTICS OF THE COILS OF PROTOTYPE MODULE

Coil No.	Inner radius (mm)	Outer radius (mm)	Length (mm)	No. of Layers	Turns/layer
14	401.2	474.7	186.7	17	17
15	401.2	478.3	186.7	18	17

III. MECHANICAL ANALYSIS

In order to calculate the stress levels in the two coils and the shell composing the prototype, it is necessary to take into account the whole history of the magnet starting from the winding. Consequently, we developed an axisymmetric model for simulating the coil winding on a removable mandrel, the vacuum impregnation and the mandrel removal. The resulting model of the coil, with internal stresses coming from the construction process, was used for simulating the shrink-fitting process and then the stress from the cool-down and energization were computed. The goal of the analysis was to optimize the mechanical interference between coil and mandrel.

The model takes into account all the details of the winding (conductor and insulation), as shown in Fig.2 where one can see the Von Mises stresses calculated after the winding, with a conductor tension of 10 MPa.

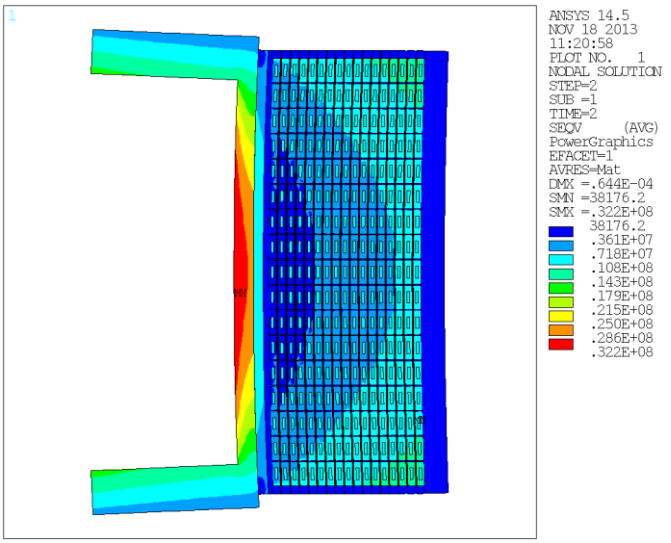

Fig. 2. Axisymmetric model for the finite element analysis (using ANSYS) of coil 14. The figure shows the Von Mises stresses and amplified deformations after the winding on a mandrel. The left C-shaped structure represents the mandrel.

This analysis requires knowledge of the mechanical material properties. We were uncertain about the material properties to be assigned to the NbTi Rutherford cable immersed in the pure aluminum matrix. Because of this, we performed computations assuming two extreme values of the Young modulus of the cable along the conductor: (a) 50-55 MPa (at room temperature and 4.2 K), i.e., equal to pure Al modulus; (b) 120-140 MPa, i.e., equal to the copper Young's modulus. In both cases the modulus was considered to have values of 90-120 MPa in the transverse direction. For the stabilizer the properties of pure aluminum were used. For the insulation the thermal and mechanical properties of glass (before impregnation) and fiber-glass epoxy (after impregnation) were considered.

After analyzing all steps of construction and cool-down we calculated the Von Mises (VM) stresses in the coil and shell for different values of the mechanical interference. We mainly looked at the cool-down because of the potential for large stresses due to differential thermal contraction. The energization introduces only a minor variation in the stresses. Figure 3 shows the VM stresses in the pure aluminum components of the conductor and in the external shell as a function of the mechanical interference at room temperature. Even with no interference a light pressure between the coil and shell takes place. However, the minimum absolute value of the shell tension (10 MPa) is too small to guarantee that no detachment of the coil-shell can occur. Since the VM stress in pure aluminum has a minimum for interferences between 0.10-0.30 mm, we decided to use a nominal interference of 0.20 mm. With this interference, heating up the shell to 120^{o}C causes a gap of 0.80 mm to open between the coils and shell, a value considered safe for the shrink-fitting operation.

A. 3D Mechanical Model

The 2D analysis presented above was complemented with a 3D analysis, simulating the complete prototype module. The model is shown in Fig. 4. The coil was modeled as a homogeneous but anisotropic medium with mechanical properties derived from an FEA of a short length of a single conductor. Cool-down and energization loads were considered, but a historical approach starting from winding as was done in the 2D analysis was not used. The magnetic forces applied to the model are the forces occurring when all Mu2e solenoids are powered.

The aim of this analysis was to check the results of the 2D analysis and to study the axial pre-stress that needs to be applied.

The main results can be summarised as follows:

a) The radial interference is highly effective in increasing the compressive hoop stress due to cool-down, with a gain of about 8 MPa per 100 μm. This result is in complete agreement with the 2D analysis.

b) Axial shimming is much less effective in increasing the compressive axial stress due to cool down. The gain is about 0.8 MPa per 100 μm

c) An uncertainty in the coefficient of thermal expansion for the coil material of ±2% causes a variation in the preload of about ±3 MPa in hoop stress

d) Axial results for even the worst case of no shimming are acceptable; average stresses are small and compressive.

e) A special condition was studied by reversing the currents and assuming that the coils are contained in a frictionless envelope. It was found that even under the frictionless condition the coil would likely unload from the shell.

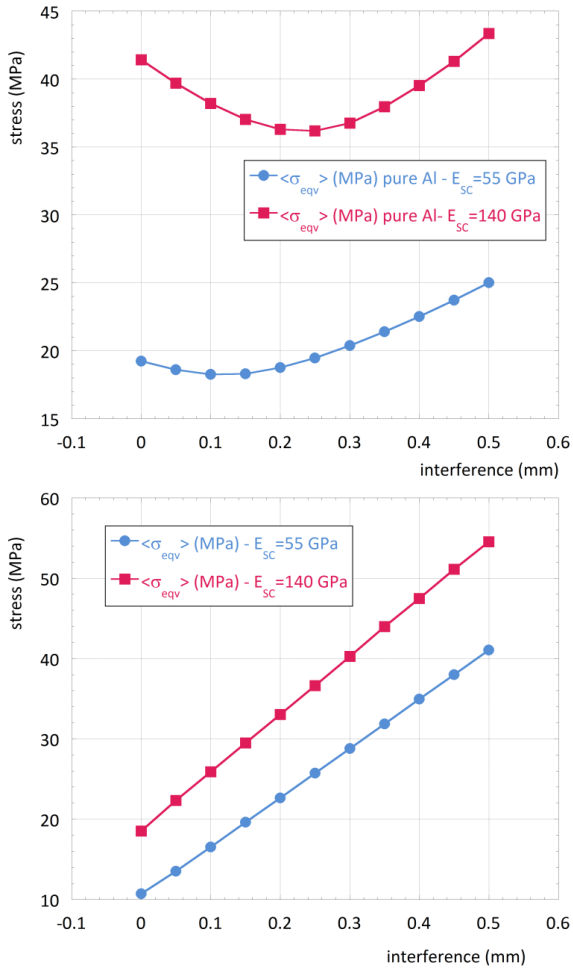

Fig.3. Von Mises average stresses after cool-down in the pure Al component of the conductor (upper) and in the Al-alloy shell (lower).

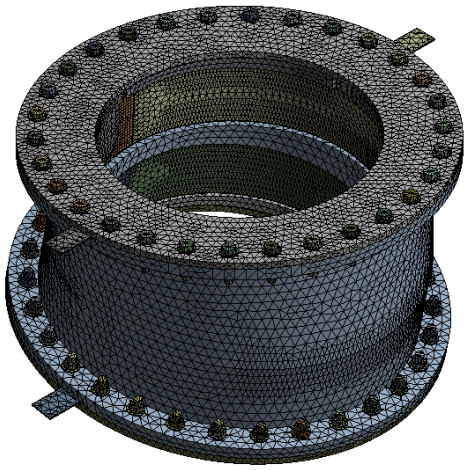

Fig. 4. The 3D meshed model of the prototype module.

The conclusion of the 3D analysis is that a 100 µm radial interference at room temperature seems prudent, whilst for the axial preloading either 0.1 mm of shimming, or no shimming, could be used.

The 0.2 mm interference coming from the 2D analysis was confirmed. We chose the more conservative 0.2 mm interference value for fabrication to cover expected geometrical machining tolerences. .

IV. Module Construction

The Italian Institute for Nuclear Physics (INFN) is in charge of the construction of the prototype module, with Fermilab providing the aluminum shell. After an international tender the contract was awarded to ASG Superconductors in Genova (I).

Figure 5 shows the cross section of coil #14. The large G10 layer on the outer radius had to be machined after impregnation in order to obtain a precise surface for the shrink-fitting operation, and it had to have nominal insulation thickness on the coil's outer surface after accommodating the tolerance of the winding process.

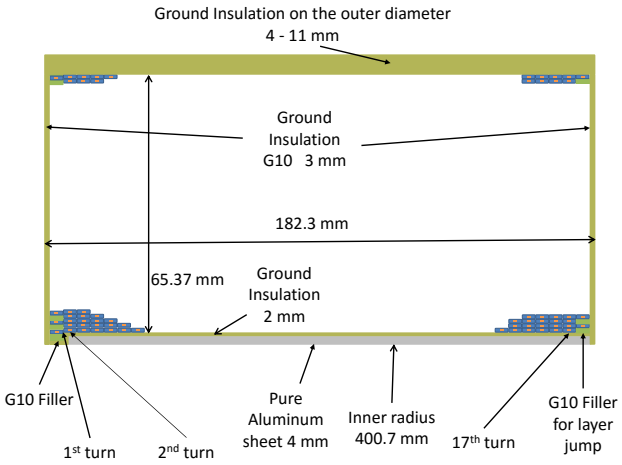

Fig. 5. Cross section of coil #14.

The two coils composing the module were wound using a prototype conductor. After resin impregnation under vacuum, the external radial surface was precisely machined. The measured external diameter of the finished coils (shown in Fig.5) is within an average oscillation of 0.05 mm of the nominal value.

Fig. 6. The two coils of the prototype module after impregnation and machining of the external surface.

The inner surfaces of the shell in contact with the coils were machined to inner radii 0.20 mm lower than the machined external coil radii. The shell was built in USA. The average

mechanical interference between the coils and shell at T=20°C is 0.167 mm for coil #14 and 0.170 mm for coil #15. These values are very close to the design value of 0.20 mm and considered acceptable. For the future we are considering an increase of the nominal interference up to 0.30 mm.

The design of the tooling for shrink fitting the coils has to solve a basic problem. For sake of simplicity and to reduce risk, one coil at a time was shrink-fitted in a very well controlled operation. During this operation the coils are at room temperature, whilst the shell temperature is kept at 120°C. In the time period between the shrink-fitting of the first and second coils, the first coil is heating up. If the temperature in first coil rises higher than 90°C (the glass transition of the epoxy), the fiberglass epoxy might lose its mechanical strength and the radial pre-stress might be greatly reduced.

To avoid this, a dedicated tool was designed to ensure that the shrink-fitting occurs within one half hour. The conceptual design of the tool is shown in Fig.7. The coils are placed on a support structure with axes normal to the ground. The shell can be moved and rotated by pneumatic actuators. The shrink-fitting is done by moving the shell downward toward the coils. After shrink-ftting the first coil, the shell is rotated and moved onto the second coil.

Fig. 7 Conceptual design of the shrink fitting tooling

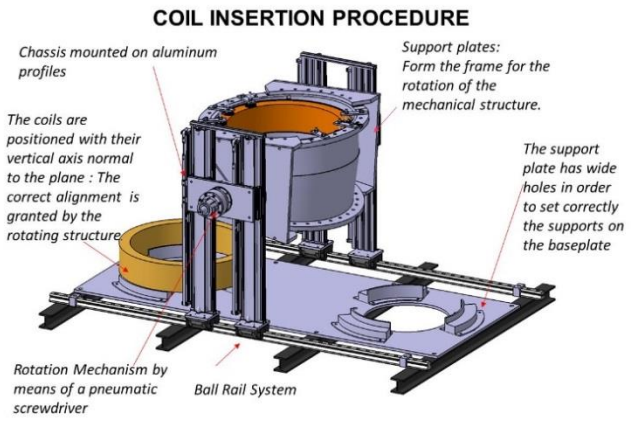

Fig. 7 Conceptual design of the shrink fitting tooling

Using this tool the coils were successfully shrink-fitted. Figure 8 shows a photograph of the actual shrink-fitting operation.

The operation lasted 20 minutes from the start of the shrink-fitting of the first coil to the completion of shrink-fitting of the second coil. After 40 minutes from the start the temperature of the mandrel fell down to 90°C with the coil at about 54°C.

The external radius of the shell was measured and compared with the values measured before the shrink fitting. The part of the shell containing coil #14 experienced an increase in diameter of 0.12 mm. The part containing coil #15 increased in diameter by 0.08 mm. This increase in shell diameter is a sign that the shell is under tension, and the shrink fitting operation had a positive result. Unfortunately, we could not compare the values of strain-gauges placed on the shell's external surface because they were damaged by the shell heating to 120°C. According to 2D mechanical computations, the expected increase in the shell diameter should have been between 0.14 mm and 0.15 mm when the interference is 0.17 mm on the radius. Consequently, for coil #14 the pre-stress is very close to expectations. For coil #15 the displacement is apparently about half the calculated one. It could be that for coil #15, the first one shrink fitted, the longer contact with the shell caused a slight weakening of the fiberglass epoxy of the ground insulation.

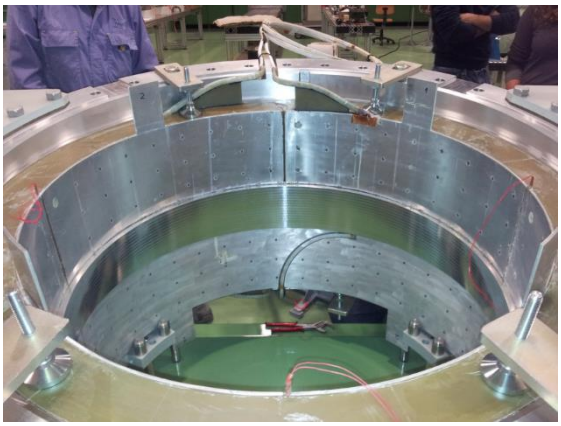

Fig. 8 Photograph of the shrink-fitting operation. This picture was taken after the first coil had been shrink-fitted, the shell rotated and placed on the second coil, being now inserted into the shell.

The finished module delivered to Fermilab is shown in Fig.9. A cold test was successfully performed in July 2015. The results of this test are reported in Ref. [8].

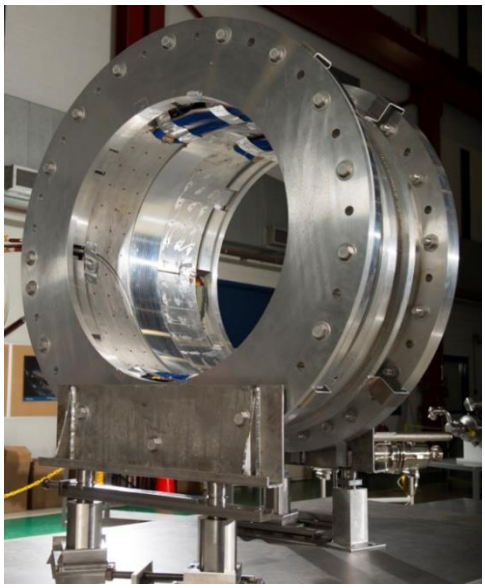

Fig. 9 The finished module delivered to Fermilab.

The construction of the prototype module demonstrates that the coils of the TS modules can be constructed with high precision and that a double shrink-fitting process is feasible and well controlled if a suitable tool is used. The results of the cryogenic tests confirmed that design and construction choices were correct, opening the way to the construction of all the TS modules.

REFERENCES

[1] Mu2e Collaboration, *Mu2e Technical Design Report*, arXiv: 1501.05241, 2014.

[2] M.J. Lamm, N. Andreev, G. Ambrosio, J. Brandt, R. Coleman, D. Evbota, V.V. Kashikhin, M. Lopes , J. Miller , T. Nicol, R. Ostojic , T. Page, T. Peterson, J. Popp , V. Pronskikh, M. Tartaglia, Z. Tang , M. Wake , R. Wands, R. Yamada, "Solenoid magnet system for the Fermilab Mu2e experiment", *IEEE Trans.Appl. Supercond*. **22**, 2012, #4100304.

[3] G.Ambrosio, N. Andreev, S. Cheban, R. Coleman, N. Dhanaraj, D. Evbota, S. Feher, V. Kashikhin, M. Lamm, V. Lombardo, M.L. Lopes, J. Miller, T. Nicol, D. Orris, T. Page, T. Peterson, V. Pronskikh, W. Schappert, M. Tartaglia, R. Wands "Challenges and Design of the Transport Solenoid for the Mu2e Experiment at Fermilab", *IEEE Trans. Appl. Supercond*. **24** ,2014, #4101405.

[4] H.Hirabayashi, "Detector Magnets In High Energy Physics", *IEEE Trans On Magnetics*, **24**, No. 2, 1988, pp 1256-1259.

[5] A.Yamamoto and T.Taylor, "Superconducting Magnets for Particle Detectors and Fusion Devices", *Reviews of Accelerator Science and Technology*, **5**, 2012, 91–118.

[6] E.Acerbi et al, "Thin and compensating solenoids for ZEUS detector", *IEEE Trans on Magnetics*, **24** , No 2, 1988, 1354-1357.

[7] H.Minemura et al., "Construction and Testing of a 3m Diameter x 5m Superconducting Solenoid for the Fermilab Collider Detector Facility (CDF) ", *Nuclear Instruments and Methods in Physics Research A238*, 1985, 18-34.

[8] M.Lopez et al., "Mu2e Transport Solenoid Prototype Tests Results", Contribution paper to MT-24 Conference, Seoul 2015.